Advances in Aircraft and Spacecraft Science, *Vol. 5, No. 5 (2018) 533-550*
DOI: https://doi.org/10.12989/aas.2018.5.5.533

Detonation transmission with an abrupt change in area

Yao-Chung Hsu[1a], Yei-Chin Chao[1b] and Kung-Ming Chung*[2]

[1]*Department of Aeronautics and Astronautics, National Cheng Kung University, 1 University Road, East district, Tainan 701, Taiwan*
[2]*Aerospace Science and Technology Research Center, National Cheng Kung University, 2500 Section 1, Chung-Cheng South Road, Guiren district, Tainan 711, Taiwan*

(Received July 18, 2017, Revised October 20, 2017, Accepted January 31, 2018)

Abstract. Detonation transmission between propane/oxygen (donor) and propane/air (acceptor) with an abrupt area change is experimentally studied. In the donor, there are two types of incident detonation waves: A self-sustained Chapman–Jouguet (CJ) detonation wave and an overdriven detonation wave that is a result of the difference in the initial donor pressure ratios. The piston work is used to characterize the strength of the incident detonation wave. For an incident CJ detonation wave, the re-initiation of a detonation wave in the acceptor depends on the initial pressure in the donor and the expansion ratio. The axisymmetric and non-axisymmetric soot patterns respectively correspond to direct detonation and detonation re-initiation. For an incident overdriven detonation wave, the re-initiation of a detonation wave in the acceptor strongly depends on the degree of overdrive.

Keywords: detonation; overdriven detonation; expansion ratio; piston work

1. Introduction

Detonation engines can be classified into two types: Intermittent type or pulse detonation engines (PDEs) (Kailasanath 2003, Fan *et al*. 2013, Pandey and Debnath 2016, Joshi and Lu 2016) and continuous detonation engines or rotary detonation engines (RDEs) (Lu and Braun 2014, Wang *et al*. 2011, Yao and Wang 2016, Yang *et al*. 2016). A PDE can perform better than conventional engines in conditions ranging from the engine being at rest to flight at a high Mach number. A detonation wave is usually initiated by a deflagration-to-detonation transition (DDT) process (Urtiew and Oppenheim 1966, Lee and Moen 1980, Moen 1993, Kuznetsov *et al*. 1997, Oran and Gamezo 2007, Ciccarelli and Dorofeev 2008, Dorofeev 2011, Alhussan *et al*. 2016). However, the DDT distance, X_{DDT}, is critical in practical applications and is mainly related to the properties of the mixture and the tube diameter, d (Li *et al*. 2006). Therefore, a detonation wave can be initiated in a relatively small tube (a pre-detonator or a donor) that contains a highly sensitive mixture and then expands to a larger tube that contains a less sensitive mixture (an acceptor). And also the presence of DDT enhancing devices. In a straight tube, Kuznetsov *et al*. (1998) found that detonation transmission depends on the properties of the two mixtures at the

*Corresponding author, Ph.D., Research Fellow, E-mail: kmchung@mail.ncku.edu.tw
[a]Ph.D., Assistant researcher
[b]Ph.D., Professor

http://www.techno-press.org/?journal=aas&subpage=7 ISSN: 2287-528X (Print), 2287-5271 (Online)

same initial pressure. A smooth diffusion zone allows successful transmission. Li *et al*. (2008) studied the effect of the degree of overdrive in an incident detonation wave on detonation transmission across a mixture. The strength of the incident overdriven detonation wave is critical to the wave transmission process.

There have been numerous studies of detonation diffraction from a donor to an acceptor (Edwards *et al*. 1979, Knystautas *et al*. 1982, Moen *et al*. 1985, Vasil'ev 1988, Pintgen and Shepherd 2009, Wu and Kuo 2012). Detonation transmission can be classified as supercritical, critical, or subcritical. In critical transmission, the precursor shock wave and the reaction wave are decoupled and several explosion bubbles occur near the centerline. A detonation is re-initiated and the donor's diameter is known as the critical diameter, d_c. Detonation transmission also depends significantly on the strength of the incident detonation wave. The critical pressure for successful detonation transmission is reduced considerably by ensuring that a donor has an optimal length or an overdriven incident detonation wave (Vasil'ev *et al*. 2006, Krivosheev and Penyaz'kov 2011).

The propagation of a detonation wave across different mixtures and through an abrupt change in area is crucial for PDEs and RDEs. However, few studies have addressed these two factors simultaneously. This study experimentally studies the detonation transmission from a donor (d = 50.8 mm) that contains a C_3H_8/O_2 mixture to an acceptor (D = 101.6 and 152.4 mm) that contains a C_3H_8/air mixture. A Chapman–Jouguet (CJ) detonation or an overdriven detonation is used as the incident detonation wave. The effect of the initial pressure and the equivalence ratio in the donor is studied. The critical conditions for detonation transmission for different initial pressures and equivalence ratios are then determined. A piston work model is also used to correlate the criteria for detonation transmission.

2. Experimental setup

2.1 Facility and instrumentation

The apparatus used in experiments is shown in Fig. 1. The tube was constructed using smooth, aluminum 6061-T6 tubes. The expansion ratios, D^* (= D/d), were 2 and 3, where D (= 101.6 and 152.4 mm) and d (= 50.8 mm) are the inner diameters of the acceptor and donor, respectively. For a stoichiometric C_3H_8/O_2 mixture, Li *et al*. (2006) demonstrated that X_{DDT} is approximately 150 mm from the closed end of a smooth tube that has a value for d value of 50.8 mm. Therefore, the length of the donor is 762 mm and the length of the acceptor is 914.4 and 457.2 mm, for D^* = 2 and 3, respectively. All of the test cases are listed in Table 1. For example, Case A_2 corresponds to an incident CJ detonation wave and Case B_2 denotes an incident overdriven wave for D^* = 2. For Case A, a thin Lumirror Mylar diaphragm (t = 30 μm) was located at 762 mm from the closed end. For Case B, the donor is divided into a driver donor (a CJ detonation wave) and a driven donor (an overdriven detonation wave) and another Mylar diaphragm was located at 584.2 mm from the close end. Note that the presence of a diaphragm induces a stronger incident detonation wave ahead of the interface of the mixtures. The diaphragm effect on post-transmission is less significant, when the thickness of a diaphragm is less than 50 μm (Li *et al*. 2015).

Prior to each run, the donor and the acceptor were evacuated to 20 Pa, using a vacuum pump (LEYBOLD PT50). C_3H_8 and O_2 were then injected into the tubes sequentially and the value of the equivalence ratio, ϕ, was determined using the partial pressure method. To ensure the homogeneity of the mixtures in the donor and the acceptor, two circulation pumps (Charles Austen EX7 and ULVAC DA-20D) were used for approximately 3 minutes. The ignition system includes a

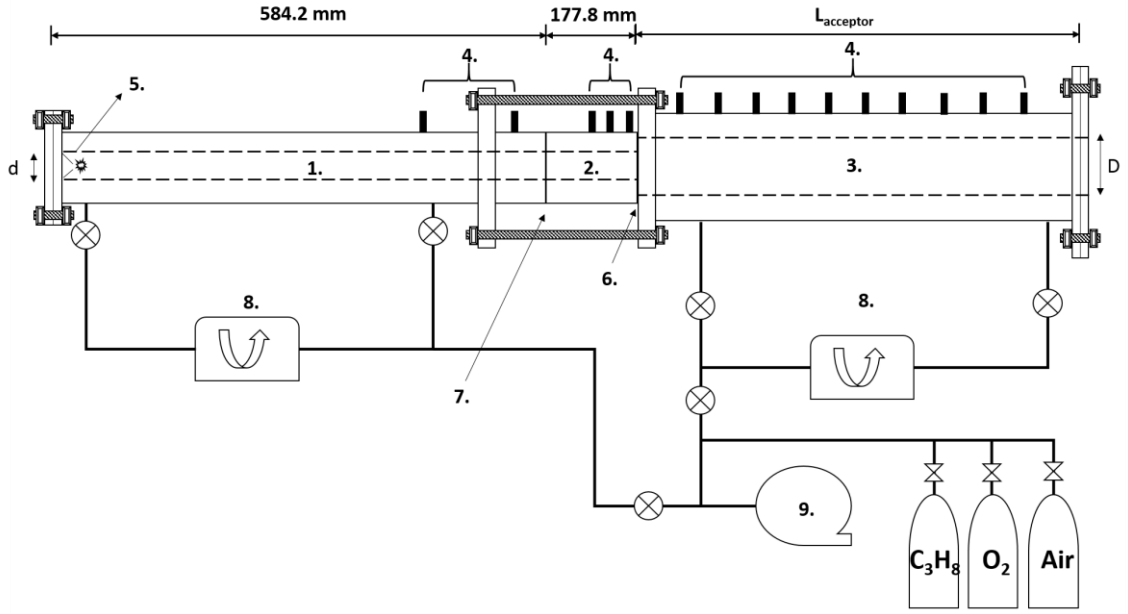

Fig. 1 Experimental setup: 1. Donor (Case A) or driver-donor (Case B), 2. Donor (Case A) or driven-donor (Case B), 3. Acceptor, 4. PCB 113B22, 5. Spark electrodes, 6. Mylar, 7. Mylar (only for Case B), 8. Circulation pump and 9. Vacuum pump

Table 1 List of test cases

Inner diameter of acceptor, *D*, mm	CJ detonation	Overdriven detonation
101.6	A_2	B_2
152.4	A_3	B_3

*The inner diameter of the donor, *d*, is 50.8 mm.

Table 2 The streamwise locations of the pressure transducers

D/d	Locations of the pressure transducers in the acceptor, m							
2	0.0381	0.0762	0.1143	0.1524	0.1905	0.2286	0.2667	0.3048
3	0.01905	0.1016	0.127	0.1524	0.2413	0.3175	0.3937	0.4699

transformer (May and Christie, z201402e2), a high voltage supply (≈ 220 V), a solid-state relay and an ignition head with two electrodes. The electrodes were made of copper and the gap between the two electrodes was 3 mm. The output from the high voltage supply was triggered by a TTL signal that was generated by a National Instruments (NI) SCXI module. The primary voltage for the transformer was 220 V; the secondary voltage was 14 kV, which was also the potential difference at the electrodes. The second voltage was measured using a high-voltage probe (HVP-15HF) and an oscilloscope (HP 54600B). The duration of the effective energy release was approximately 2 ms.

The velocity and pressure of the CJ detonation wave for a C_3H_8/O_2 mixture are calculated using STANJAN (Reynolds 1986). Both the pressure and the temperature increase when ϕ increases from 1 to 2. The maximum pressure is observed at a value for ϕ of approximately 2. Therefore, test

cases for stoichiometric and fuel-rich conditions in the donor were conducted for this study. The initial pressure in the donor, p_d, ranged from 1 to 2.5 atm. The initial pressure for the stoichiometric C_3H_8/air mixture in the acceptor was 1 atm for all test cases. The speeds of the shock and the detonation waves were measured using the time-of-flight and pressure sensors. The positions of pressure transducers are shown in Table 2. Piezoelectric pressure transducers (PCB 113B22) were installed on the tube wall. The rise time for the transducers was 1 μs. The sensors were mounted on the donor and were used to characterize the propagation of the incident detonation wave (an overdriven detonation wave or a CJ detonation wave). The velocity of the pressure wave in the acceptor was also evaluated. The propagation speed was estimated using the equation $u = \Delta L / (\Delta t \pm e_t)$, where Δt and ΔL are the propagation time for a wave past two pressure sensors and the spacing between the sensors, respectively. The uncertainty in the propagation time for a detonation wave past two pressure sensors is given by $e_t = \sqrt{e_\tau^2 + e_r^2}$, where e_τ corresponds to the error that arises from actual wave front spreading over a small time interval, instead of a step rise and e_r is the inherent rise time for the pressure transducers (Lu *et al*. 2009). The signals from the pressure transducers were acquired simultaneously and stored in NI-PXI 6133 high-speed data acquisition modules, using a sampling time of 1 μs. The report value of wave speed is the average of three shots for each test condition, where the uncertainty is estimated to be approximately 6.3%.

An easy method of measuring the cell width, λ (Strehlow 1969, Knystautas 1984, Bauer *et al*. 1986) and the structure of a transmitted detonation wave (Desbordes and Vachon 1986, Ohyagi *et al*. 2002, Sorin *et al*. 2009, Wen *et al*. 2015) involves the use of a soot track on a metal foil (or smoked foil), to visualize the propagation of a detonation wave, reflection of a shock wave and detonation re-initiation. The smoked foil was prepared by rolling 0.6-mm aluminum foils of different sizes. The size that was used depended on the size of the acceptor. A thin layer of silicone oil (Dow Corning, 50 cs) was applied uniformly on the surface of the foil. To ensure a highly uniform pasting, the foils were left for several hours until the imprint of the pasting had disappeared. Soot is then formed by burning the kerosene pool on the furnace and it is transported by the flow of burned gas onto the foil. The smoked foil fitted the inner wall of the tube well and did not interfere with the pressure transducers. After each experiment, the smoked foil was removed from the acceptor and unrolled onto a flat surface. A digital camera (Nikon D90) was used to photograph the smoked foils.

2.2 Direct initiation energy

For detonation transmission when there is an abrupt change in area, the relationship $d_c = 13\lambda$ is valid for most hydrocarbon/oxidizer mixtures. The value of d_c is directly related to the chemical properties of the mixtures. A piston work model was proposed by Lee and Matsui (1977). The critical energy for direct detonation initiation is represented in terms of the cubic diameter of the tube before the detonation arrives at the diffraction plane. This method allows predictions and experimental results to be compared. For a detonation wave that propagates across mixtures, there are two cell widths and the typical value of 13λ may not be applicable. Sochet *et al*. (1999) refined the critical energy estimation procedure by modifying the coefficients in the classical piston work model and the surface energy model. The piston work is represented as a function of the initial density, ρ_0, the specific heat ratio of the product, γ_{CJ}, the CJ velocity, D_{CJ} and d, as follows:

$$W_p = \frac{\pi}{3.47} p \frac{u}{a} d^3 \tag{1}$$

$$= \frac{\pi}{3.47}\left(\frac{\rho_0 D_{CJ}^2}{\gamma_{CJ}+1}\right)\left(\frac{D_{CJ}}{\gamma_{CJ}+1}\right)\left(\frac{\gamma_{CJ}+1}{\gamma_{CJ} D_{CJ}}\right)d^3$$

$$= \frac{\pi}{3.47}\left(\frac{\rho_0 D_{CJ}^2}{\gamma_{CJ}+1}\right)\left(\frac{D_{CJ}}{\gamma_{CJ}+1}\right)\left(\frac{\gamma_{CJ}+1}{\gamma_{CJ} D_{CJ}}\right)d^3$$

where p is the pressure, a is the sound speed and u is the velocity in stationary coordinates.

3. Results and discussion

3.1 Transmission of an incident CJ detonation wave in an expansion tube (Case A)

The *v*–*x* plot for the acceptor for Case A_2 (D = 101.6 mm and D^* = 2.0) is shown in Fig. 2, where x^* (= x/d) is the normalized streamwise distance from the closed end or the diaphragm. The value of p_d ranges from 1.00 to 2.25 atm. A CJ detonation wave is formed ahead of the diaphragm that separates the stoichiometric C_3H_8/O_2 mixture and the stoichiometric C_3H_8/air mixture. When p_d = 1.00 atm, the incident detonation wave is transformed into a shock wave and decays slightly downstream. No reinitiated detonation wave is observed within the acceptor. With the value of p_d is increased (= 1.50 atm), the speed of the transmitted shock wave increases and there is no detonation re-initiation. For a value of p_d = 1.75 atm, the speed of the transmitted shock wave is slightly less than the CJ velocity, at x^* = 0.560. The highest value for V^* is observed at x^* = 1.310 and the value decreases from this point. An overdriven detonation wave is generated at x^* = 0.560 which decays to a CJ detonation wave for a value of p_d = 2.00 and 2.25 atm. The value of V^* (= V/V_{CJ}) for 2.25 atm is slightly greater than that for p_d = 2.00 atm. Hsu *et al*. (2016) demonstrated that a reinitiated detonation wave is observed at p_d = 0.75 and 1.00 atm for D^* = 1. Therefore, when there is a change in area across a mixture, it shows that the value of p_d that is required for successful detonation transmission increases.

Previous studies show that the confinement is crucial for shock reflection, for D^* values that are less than 3 (Vasil'ev 1988). The *v*–*x* plot for D^* = 3 (Case A_3) is shown in Fig. 3. It is clear that the difference between the velocity of the transmitted shock wave and the CJ velocity is greater than that for D^* = 2. Detonation re-initiation is observed only for p_d = 2.00 and 2.25 atm. The transmitted detonation wave also decays to a shock wave during propagation downstream and then becomes a CJ detonation wave. This indicates that the critical donor pressure for the successful transmission of detonation, p_{cr}, for a stoichiometric C_3H_8/O_2 mixture increases as the value of D^* increases. The pressure profiles for the transmitted wave are also of interest. For p_d = 1.75 atm (transmitted shock wave only), Fig. 4 shows that the peak pressure decreases during the propagation of the transmitted shock wave downstream. At x^* = 1.583, the peak pressure is approximately 10 atm, which is less than the value of p_{CJ} (18 atm). Behind the leading shock, a second peak pressure is observed. This corresponds to the reflection of a hemispherical shock wave. When there is detonation re-initiation, the pressure profiles for p_d = 2.00 and 2.25 atm show similar characteristics. Shock wave reflection and a higher second peak pressure are observed. In particular, for p_d = 2.25 atm as shown in Fig. 5, the amplitude of the second peak pressure at x^* = 1.583 is greater than the value for the leading shock wave, which demonstrates that shock wave reflection plays a role for detonation re-initiation. This also corresponds to higher piston work, when there is an increase in p_d. More discussions are given in section 3.2.

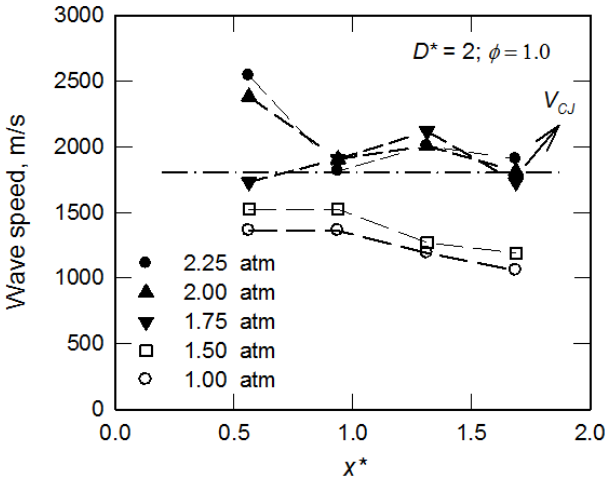

Fig. 2 The *v*-*x* plot for Case A_2: $D^* = 2$, $\phi = 1.0$

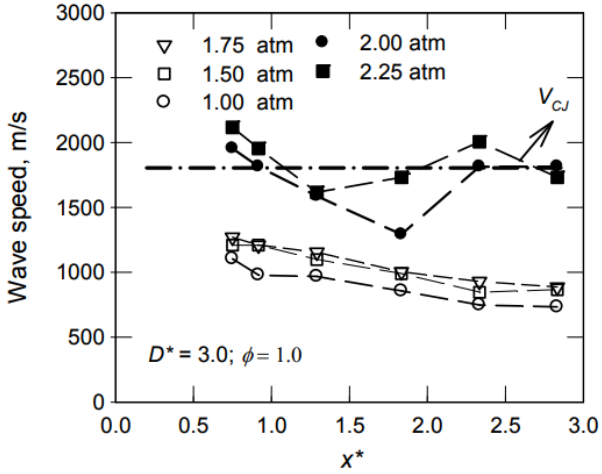

Fig. 3 The *v*-*x* plot for Case A_3: $D^* = 3$, $\phi = 1.0$

For a deflagration wave, the maximum adiabatic temperature and pressure occur for the stoichiometric condition. However, the maximum CJ velocity and the maximum pressure for a hydrocarbon mixture is typically within the fuel-rich range because the ratio of the average molecular weight of the unburned mixture to the average molecular weight of the burned product increases as the value of ϕ increases (Glassman *et al*. 2014). Therefore, if the unburned mixture has a high molecular weight, a shock wave with a high Mach number is generated. For a C_3H_8/O_2 mixture at 1 atm, the CJ pressure and velocity are calculated using STANJAN (Reynolds 1986). The maximum CJ pressure and the maximum velocity are observed around $\phi = 2$. The piston work model (Lee and Matsui 1977) shows that the energy that is provided by the piston is directly proportional to the pressure and the velocity for the burned gas, so a fuel-rich mixture in the donor allows better detonation transmission across a mixture. For $D^* = 2$ and $\phi = 2.0$, the *v*–*x* plot for the

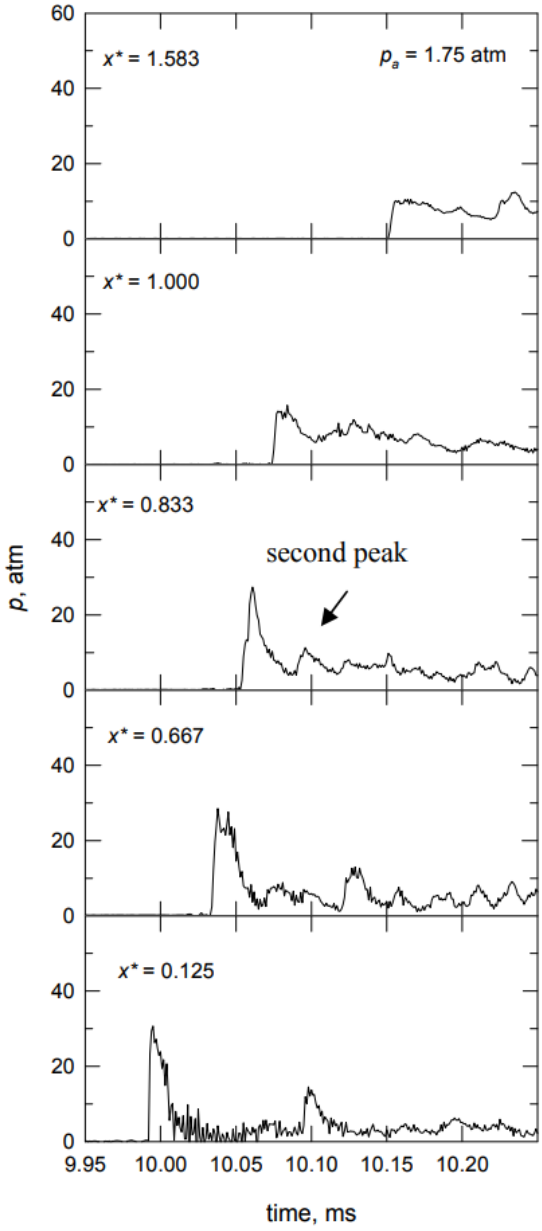

Fig. 4 The pressure profiles for Case A_3: $D^* = 3$, $\phi = 1.0$, $p_d = 1.75$ atm

acceptor is shown in Fig. 6. The speed of the transmitted shock wave for $p_d = 1.00$ and 1.25 atm is greater than that for the stoichiometric case. For $p_d \geq 1.50$ atm, detonation is reinitiated at $x^* = 0.560$ and the value of p_{cr} is reduced for a fuel-rich mixture, indicating variation of p_{cr} for different mixtures (Vasil'ev 1988).

For $D^* = 3$ and $\phi = 2.0$, the v–x plot for the acceptor is shown in Fig. 7. Decaying transmitted shock waves are observed for $p_d \leq 2.25$ atm. For $p_d = 2.50$ atm, an overdriven detonation wave is

observed for values of x^* in the range, 0.700–0.900. The wave then decays to a CJ detonation wave. Because p_{cr} is 1.50 atm for $D^* = 2$ and $\phi = 2.0$, an increase in D^* results in a high value for p_{cr} for $\phi = 2.0$. For $D^* = 3$, p_{cr} is 2.00 and 2.50 atm for $\phi = 1.0$ and 2.0, respectively. In other words, p_{cr} increases for a fuel-rich mixture. This shows an opposite trend between $D^* = 2$ and 3. Sorin *et al*. (2009) indicated that the wall reflection does not contribute to the detonation re-initiation for $D^* > 2.5$. The combined effect of ϕ and D^* on p_{cr} is worthy of further studied.

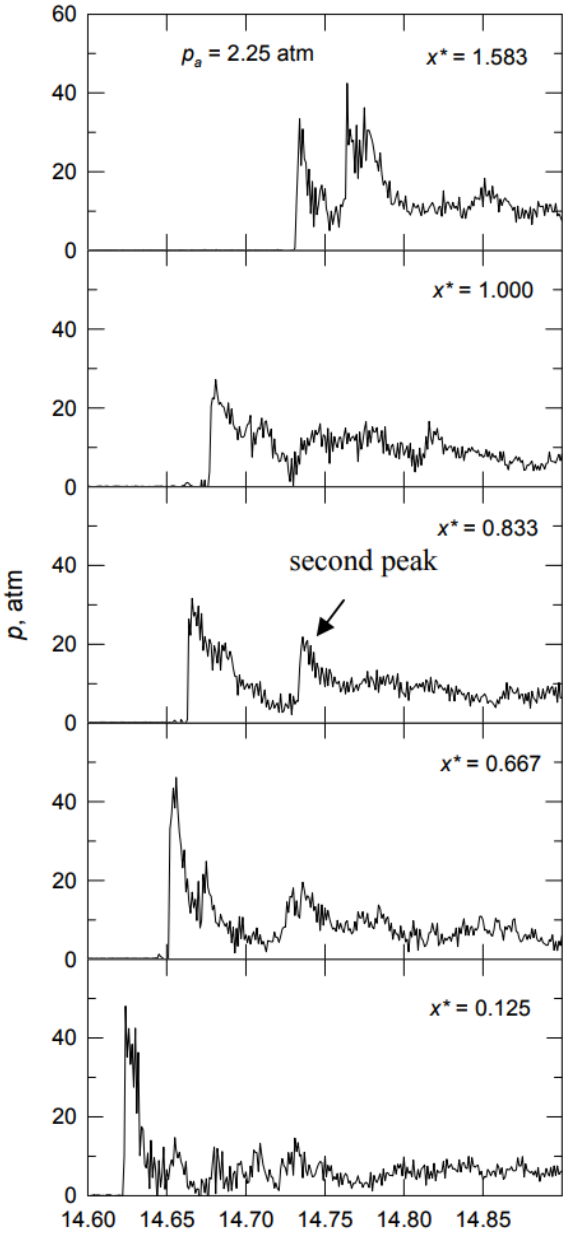

Fig. 5 The pressure profiles for Case A_3: $D^* = 3$, $\phi = 1.0$, $p_d = 2.25$ atm

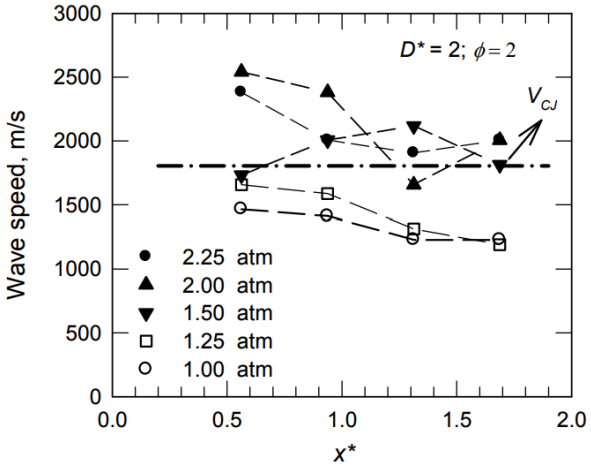

Fig. 6 The *v*-*x* plot for Case A_2: $D^* = 2$, $\phi = 2.0$

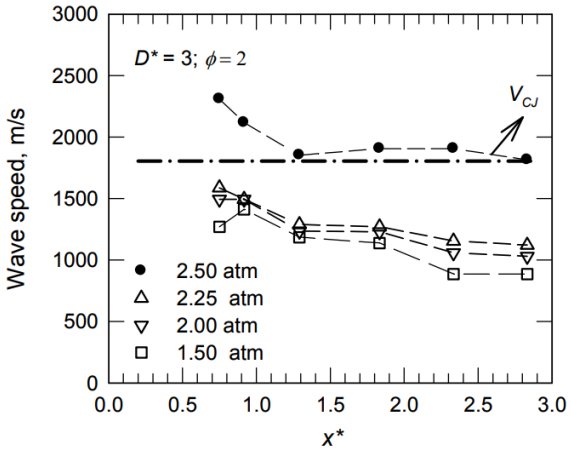

Fig. 7 The *v*-*x* plot for Case A_3: $D^* = 3$, $\phi = 2.0$

Table 3 The piston work under different initial test conditions

p_d, atm	ϕ	W_p, J
1.0	1.0	332
1.5	1.0	506
1.75	1.0	593
1.5	2.0	629
2.0	1.0	682
2.25	1.0	770
2.25	1.2	846
2.25	1.3	865
2.25	1.5	915
2.25	2.0	954
2.5	1	859
2.5	1.3	949
2.5	1.5	1020
2.5	2.0	1069

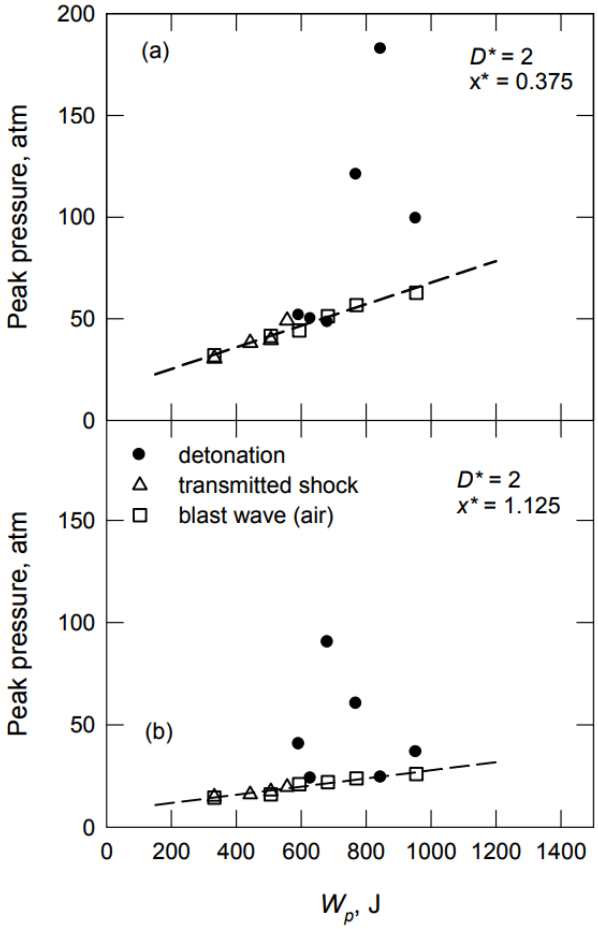

Fig. 8 Piston work versus peak wall pressure for Case A_2

3.2 The effect of piston work on detonation transmission

Detonation transmission depends on the equivalent W_p in the donor. The values of W_p (332−1069 J) for different initial test conditions in this study are listed in Table 3. For Case A_2, the peak pressure is plotted against W_p in Fig. 8. It is noted that the blast wave case corresponds to shock wave propagation in an expansion tube. When there is no detonation re-initiation (transmitted shock and blast wave), the peak pressure at $x^* = 0.375$ and 1.125 varies linearly with W_p (332−682 J). For values of W_p in the range, 593−682 J, detonation re-initiation is not observed at $x^* = 0.375$. The values of the peak pressure are approximately the same as those for transmitted shock and blast waves, so detonation is initiated at locations that are farther downstream, which is shown in Fig. 8b ($x^* \approx 1.125$). For $W_p = 770$ and 846 J, the peak pressure at $x^* = 0.375$ shows the presence of overdriven detonation waves. For $W_p = 954$ J, a decrease in the amplitude of the peak pressure means that an overdriven detonation wave is generated near the plane of the change in area ($x^* = 0$–0.375) and this decays to the CJ state rapidly within a very short distance (less than 1d). In other words, a higher value of W_p leads to an increase in peak pressure. The variation in the

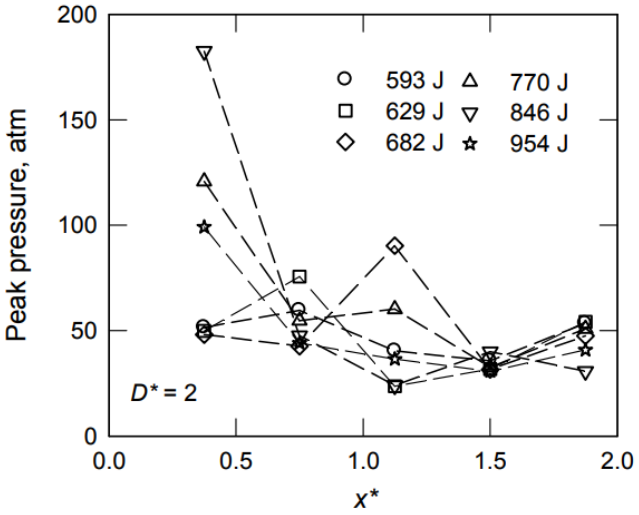

Fig. 9 The effect of W_p on peak wall pressure: Case A_2

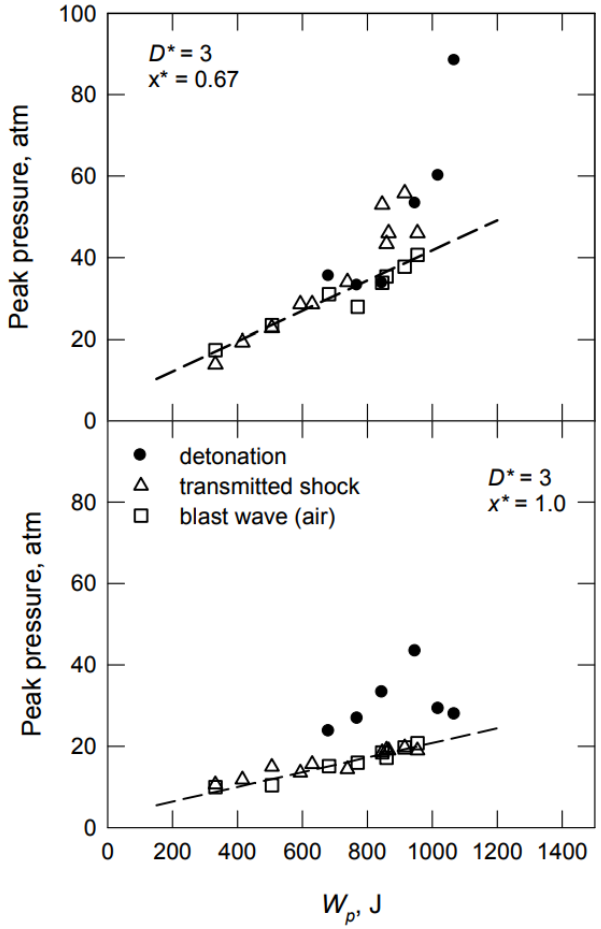

Fig. 10 Piston work versus peak wall pressure for Case A_3

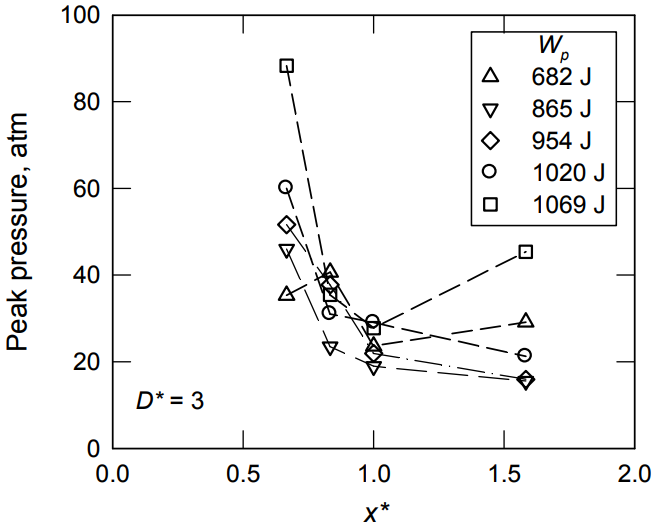

Fig. 11 The effect of W_p on peak wall pressure: Case A_3

peak pressure in the streamwise direction is plotted in Fig. 9. The peak pressures at $x^* = 0.375$ correspond to overdriven detonations for W_p values in the range, 770–954 J and these detonations are followed by the decay of the overdriven detonation waves to the CJ state. When the value of W_p is in the range, 593–682 J, a higher peak pressure is observed at locations that farther downstream, so detonation re-initiation occurs.

For $D^* = 3$, the peak pressure at $x^* = 0.670$ and 1.000 varies linearly with W_p for the test cases when there is no detonation re-initiation, as shown in Fig. 10. Detonation transmission is observed for $W_p = 1020$ and 1069 J at $x^* = 0.670$ and the overdriven detonation wave decays quickly. For $W_p \geq 682$ J, a detonation wave is re-initiated at $x^* = 1.000$. However, the peak pressure of the transmitted shock wave when the value of W_p is in the range, 846–954 J ($p_d = 2.25$ atm; $\phi = 1.2$–2.0) is greater than that for the blast wave at $x^* = 0.670$, so a fuel-rich mixture can result in an increase in the magnitude of the shock because there is a chemical reaction that involves the unburned reactive mixture behind the shock wave. Exothermal reactions supply additional piston work and corresponding shock intensification. Notably, when a blast wave from the auto-ignition kernel propagates through the unburned mixture, an overdriven detonation wave may be generated and overtake the precursor shock wave. The variation in the peak pressure in the streamwise direction for values of W_p in the range, 682–1069 J is plotted in Fig. 11. At $x^* = 0.670$, after initially decaying, the peak pressure increases with W_p.

3.3 The visualization of detonation transmission using smoked foil

The detonation transmission in the acceptor was visualized using a smoked foil. For $p_d = 2.50$ atm and $\phi = 2$ ($W_p = 1069$ J, Case A_3), an axisymmetric soot pattern, or a coupling of the shock and the reaction waves, is visible in Fig. 12. This pattern corresponds to direct detonation transmission. The bright strip indicates shock reflection at the wall. The cusp of the wave-like strip corresponds to the generation of an overdriven detonation wave, since the value of λ is comparatively small for a C_3H_8/air mixture. The wave propagates downstream in a uniform pattern in the spanwise

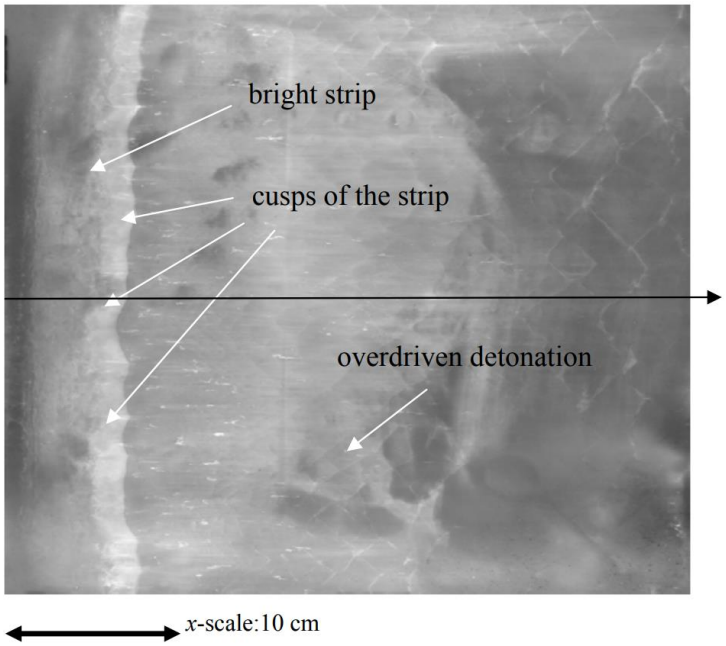

Fig. 12 The smoked foil for Case A_3: p_d = 2.5 atm, ϕ = 2

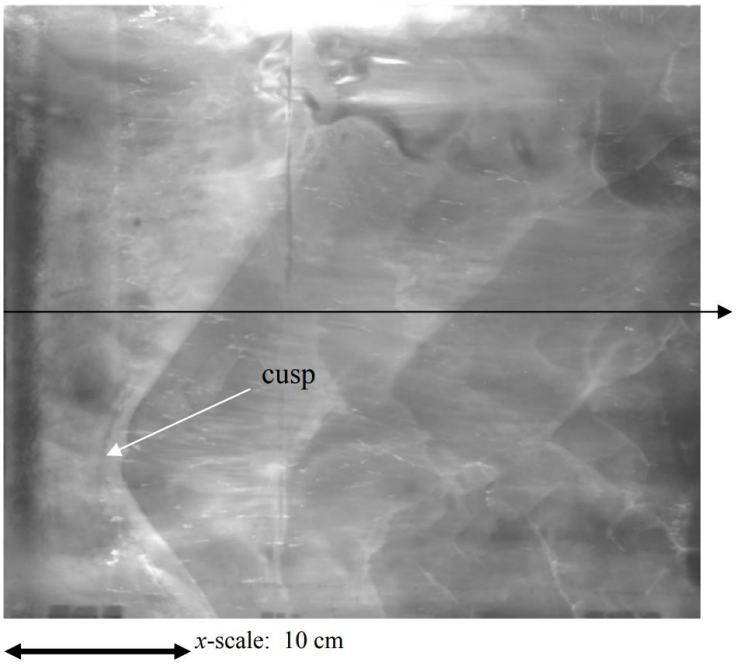

Fig. 13 The smoked foil for Case A_3: p_d = 2.5 atm, ϕ = 1.5

direction. Notably, the value of λ for an overdriven detonation wave is greater than that for a CJ detonation wave. When the piston work is decreased (p_d = 2.50 atm, ϕ = 1.3, W_p = 949 J), the soot

pattern becomes asymmetric, as shown in Fig. 13. A wave-like trace is seen near the region of shock reflection and the wavelength approaches the value of D. The cusp, which is considered to be a wave trough, is also seen on the left-lower side of the figure. This corresponds to the initiation of an overdriven detonation wave. The brush-like region probably occurs because the soot is vigorously scraped by a very-high-pressure overdriven detonation wave. On the left-upper side of the figure, a wave crest is visible. Small cells are seen downstream. This indicates that there is no steady detonation within the limited length of the acceptor and the cell structure is not well developed. For p_d = 2.25 atm and ϕ = 2.0 (W_p = 954 J), there is neither re-initiation nor detonation transmission in the region of shock reflection. However, very small cells are seen near the end of the acceptor. These are uniformly distributed in the spanwise direction. These cells occur because the presence of the end diaphragm. It means that the reflected shock wave results in high pressure and temperature, which produces a fine cell structure. For p_d = 2.25 atm and ϕ = 1.0 (W_p = 770 J), an asymmetric soot pattern is observed and a detonation wave is re-initiated. Very small cells are also observed near the end of the tube for W_p = 954 J. For Case A_2, the axisymmetric soot pattern for p_d = 2.00 and ϕ = 1.0 shows very small cells near the point where shock reflection occurs, which is similar to Case A_3 that are shown in Fig. 12. It is clearly seen that the value of λ increases in the streamwise direction, so the overdriven detonation wave weakens toward the end of the acceptor. It is also noteworthy that the piston work for Case A_3 (1069 J) is approximately 1.5 times that of Case A_2 (681 J), which demonstrates the effect of both piston work and wall confinement on detonation transmission.

On the basis of these observations, it indicates that the strength of an incident detonation wave (or piston work) is not the only factor that affects detonation re-initiation in the acceptor. For W_p = 1069 J, an overdriven detonation onsets behind the reflected shock waves, resulting in an axisymmetric soot pattern. For W_p = 770 and 1020 J, the reflected shock wave initiates an overdriven detonation wave, for which an asymmetric surface flow pattern is observed.

3.4 The effect of wall confinement on overdriven detonation transmission (Case B)

The critical pressure for successful detonation transmission across a mixture decreases when the degree of overdrive of the incident detonation wave increases. In Case B_2, a high donor pressure ratio, p_d^* (= p_{d1}/p_{d2}), value results in an increase in the degree of overdrive, where p_{d1} and p_{d2} respectively correspond to the initial pressure in the driver donor and the driven donor. For p_{d1} = 1.50 atm and ϕ = 1.0, a p_d^* value of 1.0 corresponds to the CJ condition in the driven donor and a transmitted shock wave is observed in the acceptor (no detonation re-initiation occurs in the acceptor), as shown in Fig. 14. For p_d^* = 3.0 (p_{d2} = 0.500 atm), the transmitted shock wave propagates at a speed of approximately 1500 m/s and detonation is re-initiated at x^* = 1.700. For other test cases (p_d^* = 6.5–30.0), there is detonation re-initiation and decay to the CJ state at locations that are farther downstream. Fluctuations in the propagation speed are also observed and the transmitted waves are in the CJ state at the end of the acceptor.

In Case B_2, for p_{d1} = 1.25 atm and ϕ = 1.0, if the initial pressure in the driver donor is decreased to 1.25 atm, no detonation re-initiation occurs for values of p_d^* = 2.5, 5.0 and 11.0, as shown in Fig. 15. For p_d^* = 25.0 (p_{d2} = 0.050 atm), the transmitted shock is accelerated to the CJ state at x^* ≈ 2.500. Therefore, although there is a significantly low initial pressure in the driven donor, a detonation wave is re-initiated if the value of p_d^* or the degree of overdrive are high. For Case B_3, for p_{d1} = 2.25 atm, the area ratio corresponds to the critical value for D^*. In Fig. 16, detonation re-initiation is not observed for p_d^* = 4.5, 9.0 and 15.0. A high degree of overdrive in the donor

cannot re-initiate detonation in the acceptor. Notably, the critical pressure in the donor for the CJ condition is 2 atm for $D^* = 3$. For $p_{d1} = 2.25$ atm, the CJ condition is observed at $p_d^* = 1.0$. It postulates that the minimum energy required for detonation re-initiation depends on D^* (or wall confinement).

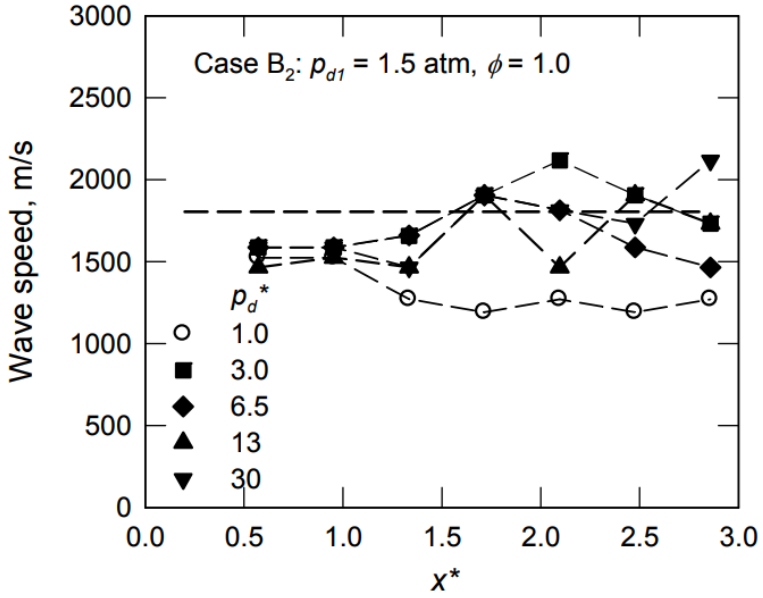

Fig. 14 The *v*-*x* plot for Case B_2: $p_{d1} = 1.50$ atm, $\phi = 1.0$

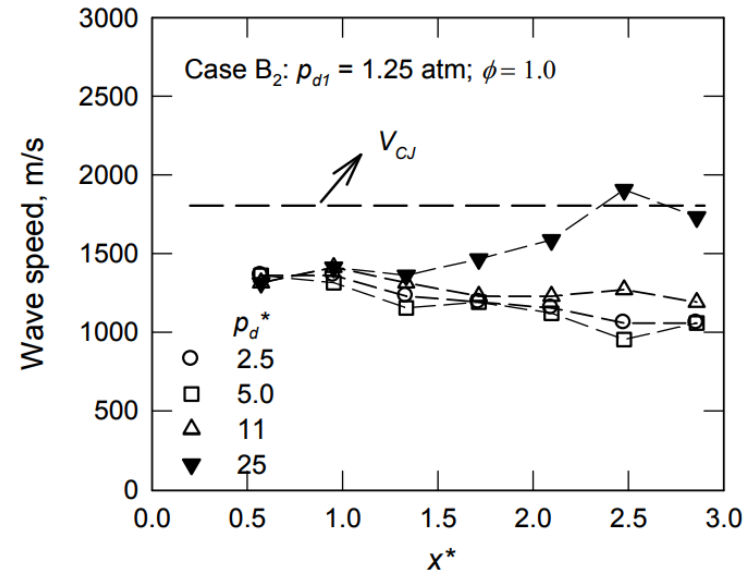

Fig. 15 The *v*-*x* plot for Case B_2: $p_{d1} = 1.25$ atm, $\phi = 1.0$

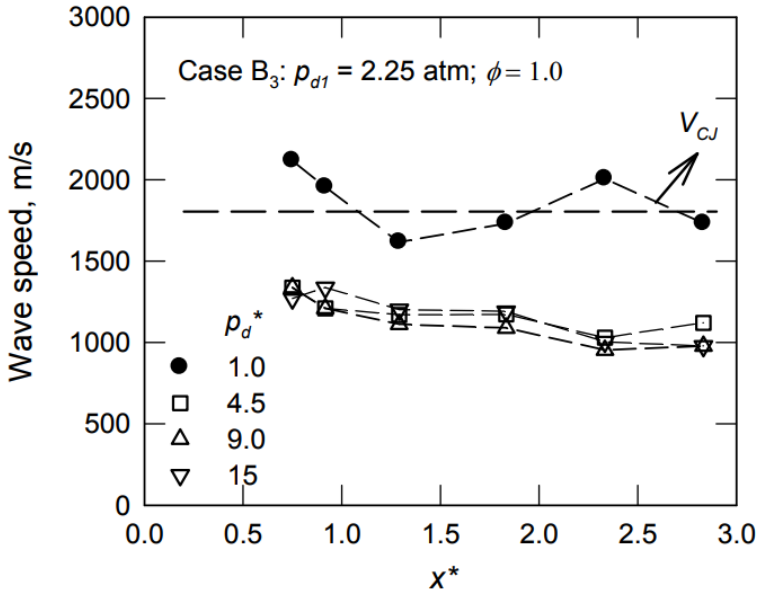

Fig. 16 The *v*-*x* plot for Case B_3: p_{d1} = 2.25 atm, ϕ = 1.0

4. Conclusions

Detonation transmission between two different mixtures when there is an abrupt change in area is studied. This occurs when there is a pre-detonator in a PDE. In expansion tubes, the incident wave must be strong, to ensure the smooth transmission of detonation. The piston work is the principal reduced variable that is used to characterize detonation transmission. Detonation transmission, including the transmitted shock, detonation re-initiation and smooth detonation transmission, is observed. This depends on wall confinement (or the expansion ratio) and the piston work. For D^* = 2, the minimum energy that is required for detonation re-initiation is 593 J. For D^* = 3, that value is 682 J. An axisymmetric soot pattern is associated with direct detonation transmission and a non-axisymmetric soot pattern is observed for detonation re-initiation.

Acknowledgments

This work was supported by the Ministry of Science and Technology (MOST 101-2221-E-006-079), Taiwan, Republic of China.

References

Alhussan, K., Assad, M. and Penazkov, O. (2016), "Analysis of the actual thermodynamic cycle of the detonation engine", *Appl. Therm. Eng.*, **107**, 339-344.

Bauer, P., Presles, H.N., Heuze, O. and Brochet, C. (1986), "Measurement of cell lengths in the detonation front of hydrocarbon oxygen and nitrogen mixtures at elevated initial pressures", *Combust. Flame*, **64**(1), 113-123.

Ciccarelli, G. and Dorofeev, S. (2008), "Flame acceleration and transition to detonation in ducts", *Prog. Energy Combust. Sci.*, **34**(4), 499-550.
Desbordes, D. and Vachon, M. (1986), "Critical diameter of diffraction for strong plane detonations", *Prog. Astro. Aero.*, **106**(1), 131-143.
Dorofeev, S. (2011), "Flame acceleration and explosion safety applications", *Proceedings Combust. Institute*, **33**(2), 2161-2175.
Edwards, D., Thomas, G.O. and Nettleton, M.A. (1979), "The diffraction of a planar detonation wave at an abrupt area change", *J. Fluid Mech.*, **95**(1), 79-96.
Fan, Z.C., Fan, W., Tu, H., Li, J. and Yan, C. (2013), "The effect of fuel pretreatment on performance of pulse detonation rocket engines", *Exp. Therm. Fluid Sci.*, **41**, 130-142.
Glassman, I., Yetter, R.A. and Glumac, N.G. (2014), *Combustion*, Academic press, MA, U.S.A.
Hsu, Y.C., Chao, Y.C. and Chung, K.M. (2016), "The initial pressure effect on detonation propagation across a mixture", *Adv. Mech. Eng.*, **8**(7), 1-9.
Joshi, D.D. and Lu, F.K. (2016), "Unsteady thrust measurements for pulse detonation engines", *J. Propulsion Power*, **32**(1), 225-236.
Kailasanath, K. (2003), "Recent developments in the research on pulse detonation engines", *AIAA J.*, **41**(2), 145-159.
Knystautas, R., Lee, J.H. and Guirao, C.M. (1982), "The critical tube diameter for detonation failure in hydrocarbon-air mixtures", *Combust. Flame*, **48**, 63-83.
Knystautas, R., Guirao, C., Lee, J.H. and Sulmistras, A. (1984), "Measurement of cell size in hydrocarbon-air mixtures and predictions of critical tube diameter, critical initiation energy and detonability limits", *Prog. Astro. Aero.*, **94**, 23-37.
Krivosheev, P.N. and Penyaz'kov, O.G. (2011), "Reducing the critical pressure of detonation initiation in transmission to a semiconfined volume", *Combust. Explos. Shock Waves*, **47**(3), 323-329.
Kuznetsov, M.S., Dorofeev, S.B., Efimenko, A.A., Alskseev, V.I. and Breitung, W. (1997), "Experimental and numerical studies on transmission of gaseous detonation to a less sensitive mixture", *Shock Waves*, **7**(5), 297-304.
Kuznetsov, M.S., Alekseev, V.I., Dorofeev, S.B., Matsukov, D. and Boccio, J.L. (1998), "Detonation propagation, decay and reinitiation in nonuniform gaseous mixtures", *Symposium on Combust.*, **27**(2), 2241-2247.
Lee, J.H. and Matsui, H. (1977), "A comparison of the critical energies for direct initiation of spherical detonations in acetylene oxygen mixtures", *Combust. Flame*, **28**, 61-66.
Lee, J.H. and Moen, I. (1980), "The mechanisms of transition from deflagration to detonation in vapor cloud explosions", *Progress Energy Combust. Sci.*, **6**(4), 359-389.
Li, J.M., Lai, W.H. and Chung, K.M. (2006), "Tube diameter effect on deflagration-to-detonation transition of propane–oxygen mixtures", *Shock Waves*, **16**(2), 109-117.
Li, J.M., Lai, W.H., Chung, K.M. and Lu, F.K. (2008), "Experimental study on transmission of an overdriven detonation wave from propane/oxygen to propane/air", *Combust. Flame*, **154**(3), 331-345.
Li, J.M., Chung, K.M. and Hau, Y.C. (2015), "Diaphragm effect on the detonation wave transmission across the interface between two mixtures", *Combust. Explos. Shock Waves*, **51**(6), 717-721.
Lu, F.K., Ortiz, A.A., Li, J.M., Kim, C.H. and Chung, K.M. (2009), "Detection of shock and detonation wave propagation by cross correlation", *Mech. Syst. Signal Pr.*, **23**(4), 1098-1111.
Lu, F.K. and Braun, E.M. (2014), "Rotating detonation wave propulsion: Experimental challenges, modeling and engine concepts", *J. Propulsion Power*, **30**(5), 1125-1142.
Moen, I., Bjerketvedt, D., Jens, A. and Thibault, P.A. (1985), "Transition to detonation in a large fuel-air cloud", *Combust. Flame*, **61**(3), 285-291.
Moen, I. (1993), "Transition to detonation in fuel-air explosive clouds", *J. Hazardous Materials*, **33**(2), 159-192.
Ohyagi, S., Obara, T., Hoshi, S., Cai, P. and Yoshihashi, T. (2002), "Diffraction and re-initiation of detonations behind a backward-facing step", *Shock Waves*, **12**(3), 221-226.
Oran, E.S. and Gamezo, V.N. (2007), "Origins of the deflagration-to-detonation transition in gas-phase

combustion", *Combust. Flame*, **148**(1-2), 4-47.
Pandey, K.M. and Debnath, P. (2016), "Review on recent advances in pulse detonation engines", *J. Combust.*, **2016**, 1-16.
Pintgen, F. and Shepherd, J. (2009), "Detonation diffraction in gases", *Combust. Flame*, **156**(3), 665-677.
Reynolds, W. (1986), "The element potential method for chemical equilibrium analysis: Implementation in the interactive program STANJAN", ME 270 HO 7; Stanford University, U.S.A.
Sochet, I., Lamy, T., Brossard, J., Vaglio, C. and Cayzac, R. (1999), "Critical tube diameter for detonation transmission and critical initiation energy of spherical detonation", *Shock Waves*, **9**(2), 113-123.
Sorin, R., Zitoun, R., Khasainov, B. and Desbordes, D. (2009), "Detonation diffraction through different geometries", *Shock Waves*, **19**(1), 11-23.
Strehlow. R.A. (1969), "Nature of transverse waves in detonations", *Astronautica Acta*, **14**(5), 539-548.
Urtiew, P. and Oppenheim, A. (1966), "Experimental observations of the transition to detonation in an explosive gas", *Proc. Royal Soc. London. Series A, Math. Phys. Sci.*, **295**, 13-28.
Vasil'ev, A. (1988), "Diffraction of multifront detonation". *Combust. Explos. Shock Waves*, **24**(1), 92-99.
Vasil'ev, A., Drozdov, M.S. and Khidirov, S.G. (2006), "Nonclassical regimes of wave diffraction in combustible mixtures", *Combust., Explos. Shock Waves*, **42**(6), 746-752.
Wang, K., Fan, W., Yan, Y., Zhu, X. and Yan, C. (2011), "Operation of a rotary-valved pulse detonation rocket engine utilizing liquid-kerosene and oxygen", *Chinese J. Aeronautics*, **24**(6), 726-733.
Wen, C.S., Chung, K.M. and Hsu, Y.C. (2015), "Smoked foil on deflagration-to-detonation transition", *J. Propulsion Power*, **31**(3), 967-969.
Wu, M.H. and Kuo, W.C. (2012), "Transition to detonation of an expanding flame ring in a sub-millimeter gap", *Combust. Flame*, **159**(3), 1366-1368.
Yang, C., Wu, X., Ma, H., Peng, L. and Gao, J. (2016), "Experimental research on initiation characteristics of a rotating detonation engine", *Exp. Therm. Fluid Sci.*, **71**, 154-163.
Yao, S. and Wang, J. (2016), "Multiple ignitions and the stability of rotating detonation waves", *Appl. Therm. Eng.*, **108**, 927-936.

CC